The CEP peptide-CRA2 receptor module promotes arbuscular mycorrhizal symbiosis

Léa Pedinotti, Juliette Teyssendier de la Serve, Thibault Roudaire, Hélène San Clemente, Marielle Aguilar, Wouter Kohlen, Florian Frugier, Nicolas Frei Dit Frey

Report

Current Biology

The CEP peptide-CRA2 receptor module promotes arbuscular mycorrhizal symbiosis

Graphical abstract

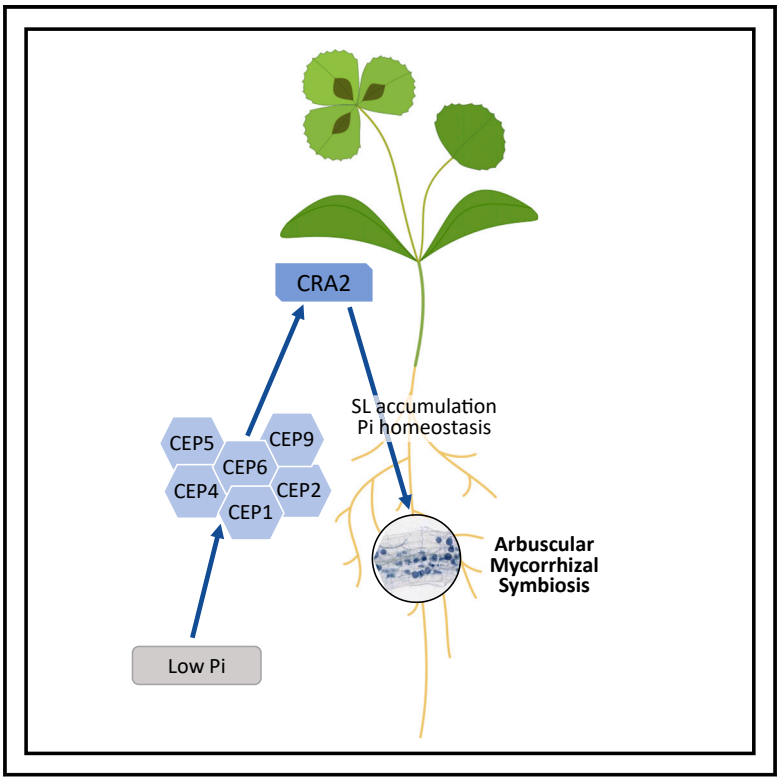

Highlights

- A subset of *M. truncatula CEP* genes is induced by low-phosphate conditions
- The CEP1 peptide positively regulates AMS establishment
- The *cra2* CEP receptor mutants display a reduced endomycorrhizal interaction
- The CEP/CRA2 pathway regulates Pi homeostasis and strigolactone accumulation

Authors

Léa Pedinotti, Juliette Teyssendier de la Serve, Thibault Roudaire, ..., Wouter Kohlen, Florian Frugier, Nicolas Frei dit Frey

Correspondence

florian.frugier@universite-paris-saclay.fr (F.F.), nicolas.frei-dit-frey@univ-tlse3.fr (N.F.d.F.)

In brief

Pedinotti and Teyssendier de la Serve et al. show that the CEP/CRA2 pathway, previously known to promote root competence to nodulate under low-nitrogen conditions in legumes, also enhances AMS establishment by controlling the expression of Pi homeostasis and strigolactone hormone biosynthesis genes, as well as strigolactone accumulation.

Pedinotti et al., 2024, Current Biology *34*, 5366–5373
November 18, 2024
https://doi.org/10.1016/j.cub.2024.09.058

CellPress

CellPress
OPEN ACCESS

Current Biology

Report

The CEP peptide-CRA2 receptor module promotes arbuscular mycorrhizal symbiosis

Léa Pedinotti,[1,5] Juliette Teyssendier de la Serve,[1,2,5] Thibault Roudaire,[3] Hélène San Clemente,[1] Marielle Aguilar,[1] Wouter Kohlen,[4] Florian Frugier,[2,*] and Nicolas Frei dit Frey[1,6,*]

[1]Laboratoire de Recherche en Sciences Végétales (LRSV), Université de Toulouse, CNRS, UPS, INP Toulouse, 31320 Castanet-Tolosan, France

[2]Institute of Plant Sciences Paris Saclay (IPS2), Paris-Saclay University, CNRS, Paris-Cité University, INRAE, Univ d'Evry, Bat. 630, Avenue des Sciences, 91190 Gif-sur-Yvette, France

[3]Laboratoire des Interactions Plantes Microbes-Environnement (LIPME), CNRS, INRAE, Université de Toulouse, 31320 Castanet-Tolosan, France

[4]Laboratory of Molecular Biology, Wageningen University & Research, Wageningen 6708 PB, the Netherlands

[5]These authors contributed equally

[6]Lead contact

*Correspondence: florian.frugier@universite-paris-saclay.fr (F.F.), nicolas.frei-dit-frey@univ-tlse3.fr (N.F.d.F.)

https://doi.org/10.1016/j.cub.2024.09.058

SUMMARY

C-terminally encoded peptides (CEPs) are small secreted signaling peptides that promote nitrogen-fixing root nodulation symbiosis in legumes, depending on soil mineral nitrogen availability.[1] In *Medicago truncatula*, their action is mediated by the leucine-rich repeat receptor-like protein kinase COMPACT ROOT ARCHITECTURE 2 (CRA2).[2–4] Like most land plants, under inorganic phosphate limitation, *M. truncatula* establishes another root endosymbiotic interaction with arbuscular fungi, the arbuscular mycorrhizal symbiosis (AMS). Because this interaction is beneficial for the plant but has a high energetic cost, it is tightly controlled by host plants to limit fungal infections mainly depending on phosphate availability.[5] We show in this study that the expression of a subset of CEP-encoding genes is enhanced in the low-phosphate conditions and that overexpression of the low-phosphate-induced *MtCEP1* gene, previously shown to promote the nitrogen-fixing root nodulation symbiosis, enhances AMS from the initial entry point of the fungi. Conversely, a loss-of-function mutation of the CRA2 receptor required for mediating CEP peptide action[2] decreases the endomycorrhizal interaction from the same initial fungal entry stage. Transcriptomic analyses revealed that the *cra2* mutant is negatively affected in the regulation of key phosphate transport and response genes as well as in the biosynthesis of strigolactone hormones that are required for establishing AMS. Accordingly, strigolactone contents were drastically decreased in *cra2* mutant roots. Overall, we showed that the CEP/CRA2 pathway promotes both root nodulation and AMS in legume plants, depending on soil mineral nutrient availability.

RESULTS AND DISCUSSION

Low phosphate availability induces the expression of a subset of *CEP* genes

To determine whether C-terminally encoded peptides (CEPs) can act in arbuscular mycorrhizal symbiosis (AMS), we analyzed the regulation of all *Medicago truncatula* (*M. truncatula*) class I *CEP* genes (Figures 1 and S1A) using RT-qPCR in arbuscular mycorrhizal fungi (AMF)-colonized roots or in contrasting inorganic phosphate (Pi) availability conditions (low Pi = 7.5 μM; high Pi = 2 mM). None of the *CEP* genes were significantly regulated upon AMF colonization (Figures 1A and S1B), despite the strong induction of the *MtPT4* mycorrhization marker (Figure S1C[6]), validating the efficient mycorrhization. In contrast, the expression of *MtCEP1*, *MtCEP2*, *MtCEP4*, *MtCEP5*, *MtCEP6*, and *MtCEP9* was significantly higher in the low-Pi condition, while *MtCEP7* was found to be weakly repressed. *Mt4*, a Pi-starvation inducible gene,[7] was used as a marker to validate that the Pi conditions were indeed contrasted (Figure S1D[8]), as also attested by the overall plant growth phenotype (Figure S1E). These results indicate that the expression of a subset of CEP-encoding genes is promoted in the low-Pi condition that is required for AMS establishment, suggesting a potential regulatory role of these signaling peptides in this symbiotic interaction. Interestingly, a role for class I CEP peptides was previously identified for another legume root endosymbiotic interaction, the nitrogen-fixing root nodule symbiosis. The regulation of these genes by Pi availability, but not by the AMS interaction by itself,[1,2] echoes the current model of the CEP-mediated regulation of nodulation by nitrogen availability.[4,9] Overall, this suggests that CEP peptides may play a role not only in symbiotic root nodulation but also in AMS in response to low Pi availability.

Overexpression of a CEP peptide enhances AMS root colonization, whereas mutation of the CRA2 receptor conversely reduces AMS

With the aim of further comparing the role of CEP peptides in both root endosymbioses, we selected *MtCEP1* among *CEP* genes responding to Pi availability, first, because it was already studied in the symbiotic nodulation context using a *p35S:MtCEP1* overexpression approach[1]; and second, because *MtCEP1* is one of the most expressed *CEP* genes in the low-Pi condition (Figure 1B). Roots overexpressing *MtCEP1* showed a significantly increased density of the different mycorrhization events quantified, from hyphal epidermal entry sites to hyphae root colonization and arbuscule formation, despite a reduced number of root apices, compared with empty vector-transformed roots (Figures 2A and S2A). Overall, this indicates that in addition to their known roles as positive regulators of nodulation[1,2] and as negative regulators of lateral root development,[1] MtCEP1 peptides also promote AMS. We additionally tested the mycorrhizal phenotype of *MtCEP2*-overexpressing roots, a CEP-encoding gene also induced by low Pi with a high fold change but reaching an overall expression level lower than *MtCEP1* (Figure 1B). Similarly, as for *CEP1* overexpression, an increased number of infection points were observed, which however did not translate into an increased overall colonization of roots by the fungi (Figure S2B). This suggests that the different *CEP* genes accumulating in low-Pi conditions might have, beyond the regulation of the initial fungi entry points in roots, differential functions on later mycorrhizal stages. As CEP peptides act through the Compact Root Architecture 2 (CRA2) receptor in *M. truncatula*,[2–4] we additionally analyzed the mycorrhization phenotype of *cra2* mutants. In both *cra2*-11 (hereafter called *cra2*) and *cra2*-1 alleles, respectively generated in the Jemalong A17 or the R108 genotype, the mycorrhizal colonization was similarly reduced (Figure S2C). Moreover, a detailed phenotyping of *cra2*-11 mutants revealed that epidermal entry sites, infection points, hyphae, and arbuscule rates were all reduced, compared with wild-type (WT) plants (Figure 2B), while the lateral root number was increased in the mutant (Figure S2A), as expected.[10] Careful observation of arbuscules using confocal microscopy, however, did not reveal major differences between *cra2* mutant and the WT (Figure S2D). This suggests that although *cra2* mutants display less colonization events, once the mutant hosts the fungus for nutrient exchanges, it is able to achieve arbuscule development similar to that in the WT. When normalizing the AMF colonization by the number of lateral roots, the mycorrhization phenotype of the *cra2* mutant was even increased, compared with WT plants (Figure 2C). The increased number of young lateral roots, and thus of susceptible regions to AMF,[11] would be expected to increase its AMF colonization rate. In contrast, the opposite result is observed, indicating even more convincingly than without normalization that the *cra2* mutant has a very low competency to interact with the AMF. Of note, the same occurs for symbiotic nodulation: despite having more lateral roots containing young regions above root tips that are the most responsive to rhizobia nitrogen-fixing bacteria, the *cra2* mutant forms nearly no symbiotic nodule.[10] As expected,[1] and antagonistically to the *cra2* mutant, *MtCEP1*-overexpressing plants displayed a decreased number of root apices (Figure S2A), consequently leading to amplifying the increase in AMF colonization when normalized to the lateral root number (Figure 2C). As the different stages of AMS were impacted, either by the *MtCEP1* overexpression or by the *CRA2* loss-of-function mutation, this suggests that the CEP/CRA2 receptor pathway is required to promote the establishment of AMS from the earliest infection stage, similarly as previously highlighted for the nitrogen-fixing symbiotic nodule initiation.[3,9] This thus represents another example of the likely evolutionary recruitment of a more ancient regulatory pathway promoting AMS for the regulation of the more recently evolved nitrogen-fixing root nodule endosymbiotic interaction.[12] Such recruitment may have also involved a potential rewiring of *CEP* gene regulation, depending on different environmental inputs, as previously documented for the nodule inception/NIN-like protein (NIN/NLP) regulatory genes in the context of symbiotic nodulation.[13,14] As *CEP* genes are induced by low-nitrogen as well as low-Pi environments, they might coordinate the root competency for both symbioses, depending on the combination of nutrient availabilities in the soil.

The nodulation-related miR2111 shoot-to-root systemic effector is not regulated by Pi availability or mycorrhization

Because of the previously characterized conservation of the CEP/CRA2 pathway regulatory function in promoting the two root endosymbioses in legumes, we then wanted to evaluate the potential involvement of the microRNA (miRNA) miR2111 downstream effector that is key to regulating nodulation, depending on nitrogen availability.[4,15] This miRNA negatively impacts the transcript accumulation of the *Too Much Love 1* and *2* (*TML1* and *TML2*) genes that act in roots as inhibitors of nodulation initiation.[4,16,17] In *M. truncatula* roots, transcript accumulation of miR2111, as well as of *TML1* and *TML2*, was not significantly regulated either in response to AMS or to Pi availability (Figure S3). Knowing that in response to nitrogen availability and rhizobium, the miR2111/TML regulatory module is rapidly and strongly regulated through the CRA2 receptor,[4] the Pi availability and AMS expression pattern of the *miR2111* and *TML* genes do not favor a role of this downstream CEP/CRA2-dependent module in the regulation of AMS. This therefore suggests that even though there is an evolutionary conservation of the CEP/CRA2 pathway to promote both root endosymbioses, downstream components have likely diverged.

The CRA2 pathway is required for regulating a subset of Pi-related and AMS-responsive genes, as well as of SL accumulation

To identify downstream molecular targets of the CEP/CRA2 pathway recruited for regulating AMS, an RNA sequencing (RNA-seq) analysis was performed to compare the root response with AMS between WT plants and *cra2* mutants. A principal-component analysis revealed clear-cut discrimination between non-mycorrhized (NM) and AMS samples, as well as between *cra2* and WT plants (Figures S4A and S4B). Globally, under low-Pi NM conditions promoting AMS, 1,218 genes showed an increased expression and 923 a decreased expression in *cra2* roots, compared with WT roots (Table S1). In agreement to the root phenotype of the mutant,[3,10] 22% of the genes

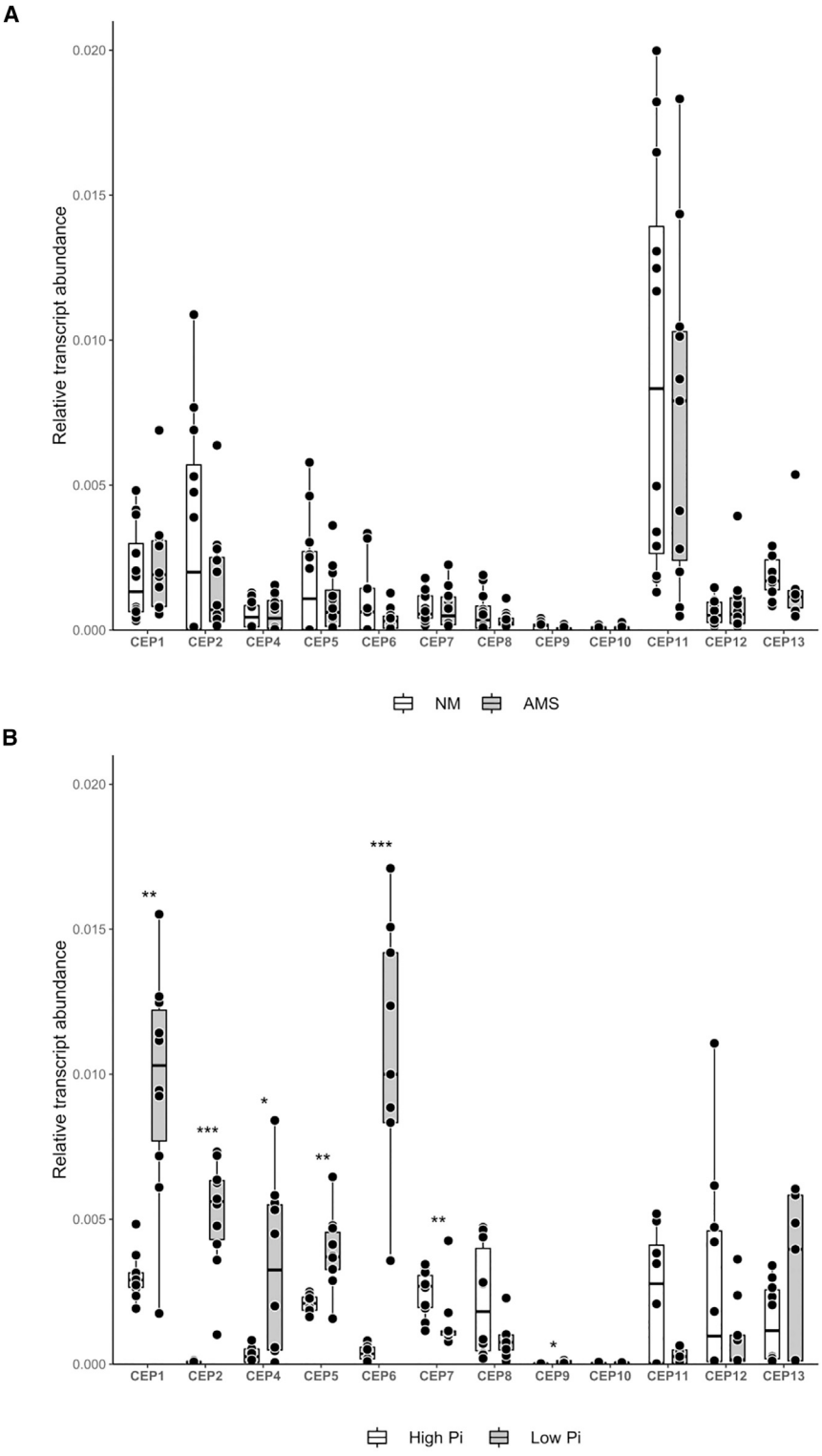

Figure 1. A subset of *MtCEP* genes is upregulated in low-Pi conditions

(A) RT-qPCR analysis of class I *MtCEP* gene expression with arbuscular mycorrhizal symbiotic (AMS) fungus inoculation or without (non-mycorrhized [NM]). A Wilcoxon test performed between the two conditions (AMS and NM) revealed no significant difference for each gene ($p < 0.05$).

(B) RT-qPCR analysis of class I *MtCEP* gene expression in low- and high-Pi conditions. A Wilcoxon test was performed between the two conditions (low and high Pi): $^{*}p < 0.05$; $^{**}p < 0.01$; $^{***}p < 0.001$.

Data from two independent biological experiments are shown ($n = 5$ pools of 3 plants per experiment). Boxes represent the middle 50% of the values, the median is represented by a horizontal line and upper and lower quartiles by vertical lines. Expression values were normalized to the *MtACT11* gene.

See also Figures S1 and S3 and Table S4.

more highly expressed in *cra2* are associated to lateral root formation (Figure S4C; Table S2;[18]). Likewise, the expression of a subset of genes related to auxin transport and responses, cell cycle, and root development was altered in the *cra2* mutant (Figures S4D and S4E). In the NM condition, some of these auxin-related genes—and notably *MtYUC2* (*Yucca 2*), an auxin biosynthesis gene—were previously reported as being similarly induced in *cra2*[19] (Figure S4D). A survey of Gene Ontologies (GOs) revealed that GO terms related to detoxification and reactive oxygen species responses were enriched for genes more highly expressed in *cra2* mutant roots, while GO terms related to cell wall biogenesis processes were enriched for genes that are more lowly expressed in *cra2* (Figures S5A and S5B), as previously documented.[19] In AMF-colonized roots, 80% and 69% of the genes that were upregulated or downregulated by AMS, respectively, are similarly regulated in *cra2* and in the WT (Figures 3A, S5C, and S5D). This correlates with the observation that *cra2* mutants engage AMS as in WT plants (Figure 2B), from the infection stage to the propagation of intraradical mycelium and arbuscule formation, even though its overall colonization rate is reduced. The remaining genes regulated by AMS in the WT and that have lost their regulation in the *cra2* mutant show an enrichment for GOs related to amino acids and RNA metabolism, respectively, for AMS-upregulated and -downregulated genes (Figures S5C and S5D). Among these, a subset of genes, once more related to auxin signaling and transport, cell cycle, and root development, is no longer regulated by AMS in *cra2* mutant roots (Figure S4E).

Focusing on genes already known to regulate AMS, a subset of these symbiotic genes has a lower expression in *cra2* mutant roots, compared with the WT already in the NM condition,

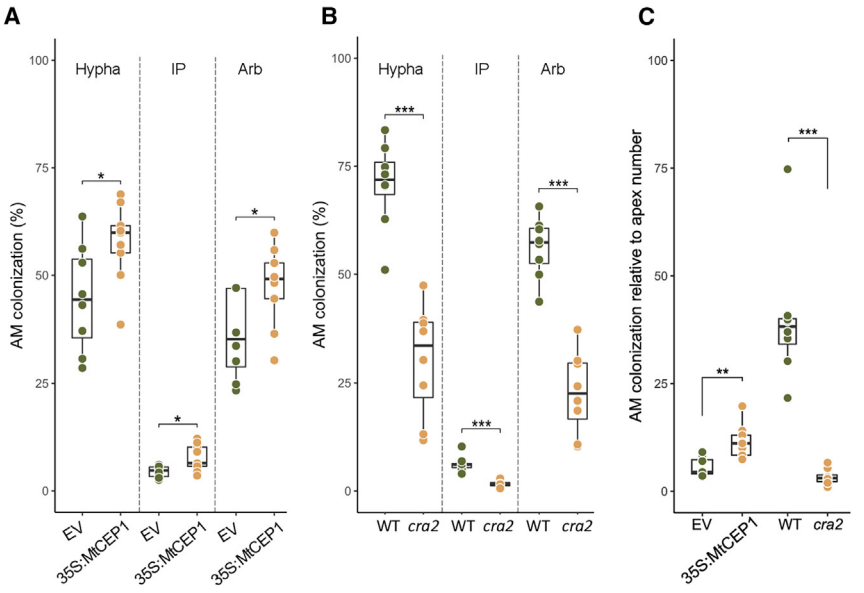

Figure 2. Mycorrhization phenotypes of roots overexpressing *MtCEP1* and of the *cra2* mutant

(A) Mycorrhizal phenotype of *MtCEP1*-overexpressing (*35S:MtCEP1*) roots and of empty vector (EV)-transformed control roots. A Wilcoxon test was performed between the two genotypes (control EV and *35S:MtCEP1*): $^{*}p < 0.05$.

(B) Mycorrhizal phenotype of *cra2* mutant and wild-type (WT) roots. A Student's t test was performed between the two genotypes (WT and *cra2*-11 mutant): $^{***}p < 0.001$.

Hypha, intraradical mycelium; IP, infection points (fungal entry sites); Arb, arbuscules.

(C) Mycorrhizal phenotype of *MtCEP1* overexpression (*35S:MtCEP1*), EV control, *cra2* mutant, and WT roots, relative to their number of root apices. The percentage of hyphal colonization was normalized to the percentage of apices in each root system (shown in Figure S2A). A Wilcoxon test was performed between the two genotypes (WT and *cra2*-11 mutant or *35S:MtCEP1*-expressing plants and EV control plants): $^{**}p < 0.01$; $^{***}p < 0.001$.

(A–C) Data represent a representative experiment ($n = 8$ plants per condition) out of three independent experiments. Boxes represent the middle 50% of the values, the median is represented by a horizontal line and upper and lower quartiles by vertical lines. See also Figure S2.

including *Reduced Arbuscular Mycorrhization 2* (*MtRAM2*), a gene encoding a lipid biosynthetic enzyme required for lipid delivery to symbiotic fungi,[22,23] and the presumed lipid transporter *stunted arbuscules 2* (*MtSTR2*) proposed to deliver these lipids to the fungus during AMS[23,24] (Table S3). In addition, the *Super Numeric Nodules* (*SUNN*) gene has an increased expression in NM roots in the *cra2* mutant, compared with the WT (Table S3). SUNN is a leucine-rich repeat receptor-like protein kinase that has been shown previously to repress AMS through the inhibition of the strigolactone (SL) hormonal pathway.[20,25] Moreover, in AMF-colonized roots, *SUNN* also shows an increased expression in *cra2,* compared with the WT, while in contrast, it shows a repression in WT AMS-colonized roots compared with NM roots (Table S3), suggesting that the CEP/CRA2 pathway may mediate a negative feedback regulation on *MtSUNN* expression.

A number of genes related to SL transport and biosynthesis were more lowly expressed in roots of *cra2* mutant plants grown in the NM condition, compared with WT roots (Figure 3B). Moreover, in the same condition, a subset of genes involved in the Pi-starvation response[26] was also expressed at lower levels in *cra2* mutant roots than in WT roots (Figure 3B). Interestingly, most of these genes show a similarly altered expression pattern in roots overexpressing *MtCLE53* (Figure 3B), a CLE peptide acting through SUNN to inhibit SL biosynthesis and thus AMS.[20] Even more strikingly, this altered *cra2* mutant Pi-starvation and SL response was maintained in AMF-colonized roots, such as for the carotenoid cleavage dioxygenase 8 (*MtCCD8*-1), *MtD27* (DWARF27), and 1-deoxy-D-xylulose-5-phosphate synthase 2 (*MtDXS2*) enzymes that act at early (MtDXS2) or late steps (MtCCD8-1, MtD27) of SL biosynthesis (Figure 3B). These results, combined with the previously documented SUNN-mediated inhibition of AMS associated to an altered regulation of SL biosynthesis,[20,25] suggest that SUNN and CRA2 antagonistically regulate AMS by modulating SL biosynthesis. To identify additional downstream targets showing SUNN-dependent and CRA2-dependent antagonistic regulations in the AMS context, we then identified the gene set that is upregulated in *cra2* and downregulated in *sunn* in AMS roots, using the Karlo et al. dataset.[25] Unexpectedly, genes associated with defense and salicylic acid-mediated GO terms were significantly enriched (Figure S5E; Table S5). In addition, genes related to Pi transport and metabolism were the most enriched GO terms among the set of genes that is downregulated in *cra2* and upregulated in *sunn* during AMS (Figure S5F; Table S5), further indicating that the antagonistic regulation of AMS by CEP/CRA2 and CLE53/SUNN pathways is tightly linked to the regulation of Pi homeostasis.

As SL production is upregulated in response to Pi-starvation conditions,[26] this RNA-seq analysis strongly suggests that the *cra2* mutant may be impaired in activating a proper Pi-starvation response. In agreement, a subset of genes relative to Pi transport, the Pi transporters 1 (*MtPT1*) and 3 (*MtPT3*), showed a higher expression in *cra2* in the NM condition and remained high in AMS roots, while they are, in contrast, repressed by AMS in the WT (Figure 3B). Interestingly, two of the three paralogs of phosphate 2 (*PHO2*), *MtPHO2-B* and *MtPHO2-C*,[27] encoding E2 enzymes that are master regulators of Pi acquisition through promoting the ubiquitination and subsequent degradation of Pi transporters and that are strongly repressed by Pi starvation,[27,28] show a higher expression in *cra2* mutant AMS roots, compared with the WT (Figure 3B). In *M. truncatula*, the repression of *PHO2* expression by AMS was previously proposed to impede the downstream regulation of Pi acquisition in root cortical cells accumulating high Pi amounts due to symbiotic exchanges.[29] Finally, it is also worth mentioning that neither the Phosphate Response 2 (*MtPHR2*) or SYG1/Pho81/XPR1 (*SPX*) Pi-sensing genes nor the Nodulation Signaling Pathway 2 (*MtNSP2*)[30–32] MtPHR2 downstream target, which were recently shown in *M. truncatula* as well as in rice[33] to be required for the Pi-starvation

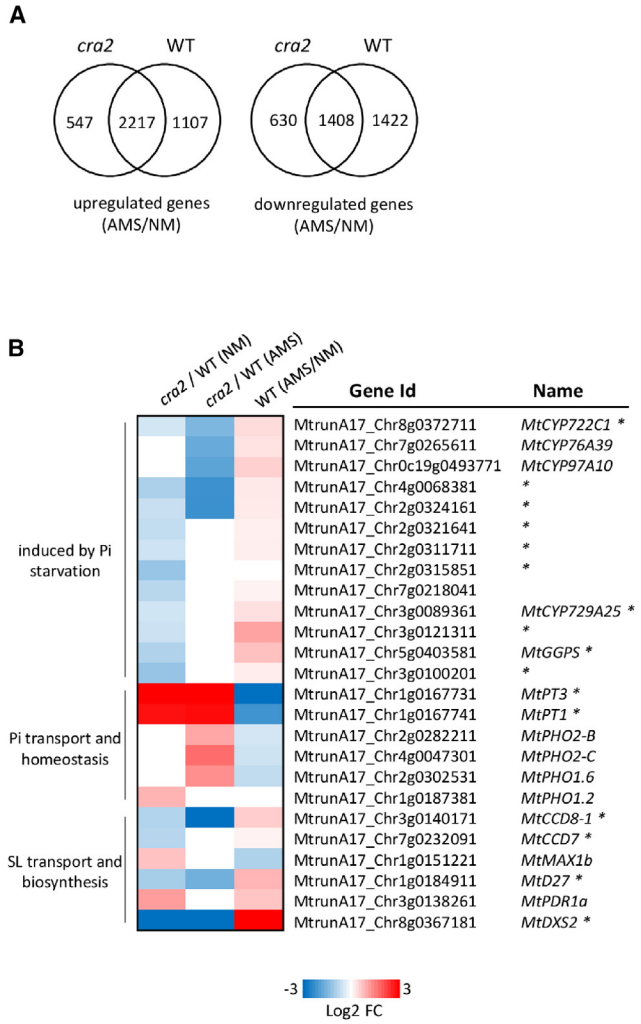

Figure 3. Regulation of selected phosphate- and strigolactone-related genes in WT versus *cra2* mutant roots

(A) Venn analysis of upregulated or downregulated genes (left or right, respectively) in 6-week-old arbuscular mycorrhizal symbiotic (AMS) colonized roots relative to non-mycorrhized (NM) roots of wild-type (WT) or *cra2* mutant plants.

(B) Heatmap of the expression pattern of strigolactone (SL) biosynthesis and transport, or Pi-starvation response, transport, or biosynthesis genes, misregulated in *cra2* mutant roots compared with the WT in NM and/or AMS conditions. Genes followed by an asterisk are also misregulated in *35S:MtCLE53* overexpressing roots[20] the same way as in *cra2* NM roots. Gene annotations from the LeGOO database were used.[21] All displayed fold changes are statistically significant (false discovery rate [FDR] < 0.05).

See also Tables S1, S2, S3, and S5 and Figures S4 and S5.

activation of SL biosynthesis in response to AMS colonization,[26] are misregulated in the *cra2* mutant (Table S1).

As SL biosynthesis genes were lowly expressed in the *cra2* mutant, we determined whether SL levels could be affected in *cra2* mutant roots grown in Pi starvation. An SL quantification revealed that didehydro-orobanchol accumulation, also known as medicaol, a potent activator of AMF hyphal branching,[34] was strongly reduced in *cra2* mutant roots (Figure 4A). This result corroborates the reduced expression of SL biosynthesis genes in the mutant. As SLs are major plant root exudate components activating AMF hyphal branching[35] and thus allowing AMS,[36] these data suggest that the reduced AMS colonization events observed in *cra2* mutant roots may be related to its inability to release sufficient amounts of SL in the rhizosphere. To test this hypothesis, *cra2* mutant and WT root exudates were applied to the seeds of the parasitic plant *Phelipanche ramose*, which require rhizospheric SLs as a germination-promoting signal to efficiently infect their hosts.[37] While WT root exudates, or the GR24 synthetic SL control, triggered the induction of *P. ramosa* seed germination, as expected, *cra2* mutant root exudates were nearly inactive (Figure 4B and S6). This result is in agreement with previous reports showing that mutants unable to produce SLs are unable to stimulate *P. ramosa* seed germination.[30,36] It also indicates that *cra2* mutant roots not only accumulate less SLs but that they are also exuding much less SLs in their rhizosphere. Overall, this could likely explain the low ability of *cra2* mutant roots to establish AMS.

In the symbiotic nodulation context, the activation of the CEP/CRA2 pathway in low-mineral-nitrogen conditions, which are required for initiating the nitrogen-fixing symbiotic interaction independently of the rhizobium microsymbiont, revealed its role in determining the root competence to nodulate, depending on host plant needs, i.e., only when mineral nitrogen availability is limited.[4,17] Similarly, the activation of the CEP/CRA2 pathway in low-Pi conditions independently of AMF colonization likely reflects its role in promoting root competence for initiating AMS, depending on host plant metabolic needs. In addition, the transcriptomic and SL quantification data suggest that this Pi-starvation promotion of AMS by the CEP/CRA2 pathway would mainly rely on the regulation of (1) the expression of a subset of Pi transport and response genes, as well as of (2) SL biosynthesis genes and thus SL accumulation and exudation into the rhizosphere. Noteworthy, the CEP-CRA2 pathway might promote AMS through an independent pathway as the previously characterized AMS-promoting SPX/PHR2/NSP2 module.

RESOURCE AVAILABILITY

Lead contact

Further information and requests for resources and reagents should be directed to and will be fulfilled by the lead contact Nicolas Frei dit Frey (nicolas.frei-dit-frey@univ-tlse3.fr).

Materials availability

All unique/stable reagents generated in this study are available from the lead contact without restriction.

Data and code availability

- The RNA-seq datasets supporting the current study have been deposited in the NCBI/SRA public repository under the accession number NCBI SRA: PRJNA1156341.
- This paper does not report original code.
- Any additional information required to reanalyze the data reported in this paper is available from the lead contact upon request

ACKNOWLEDGMENTS

Work in the F.F. laboratory was supported by the Centre National de la Recherche Scientifique (CNRS), the SYMPA-PEP project from the French Agence Nationale de la Recherche (ANR), and the Ecole Universitaire de Recherche (EUR) Saclay Plant Science (SPS). Work in the N.F.d.F. laboratory

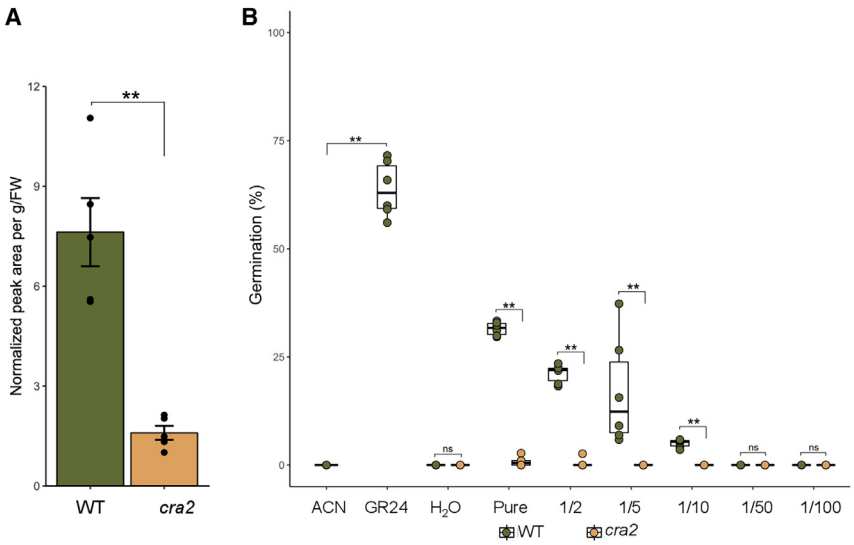

Figure 4. Strigolactones quantification in *cra2* mutant roots and *P. ramosa* seed germination in response to *cra2* root exudates

4-week-old wild-type (WT) and *cra2* mutant plants were grown under low-Pi conditions. Five pools of 3–5 root systems were then sampled for didehydro-orobanchol quantification (A), or a pool of five plants was transferred for 24 h in sterile water to collect the root exudates and perform *P. ramosa* seed germination assays (B). ACN, acetonitrile 0.001%; GR24, rac-GR24 10^{-7} M; pure, undiluted root exudates; 1/x: serial dilutions of pure root exudates with sterile water. Boxes represent the middle 50% of the values, the median is represented by a horizontal line and upper and lower quartiles by vertical lines. A Student's t test was performed between WT and *cra2* plants (A): $^{**}p < 0.01$; and a Wilcoxon between WT and *cra2* plants (B): $^{**}p < 0.01$. ns, non-significant.

See also Figure S6.

was supported by the CNRS, the SYMPA-PEP ANR project, the Fédération de Recherche Agrobiosciences, Interactions et Biodiversité (FRAIB), and the University Paul Sabatier (UPS) of Toulouse. We thank Jean-Bernard Pouvreau (Nantes University, US2B) for the gift of *P. ramosa* seeds.

AUTHOR CONTRIBUTIONS

F.F. and N.F.d.F. designed the study; L.P., J.T.d.I.S., T.R., W.K., and N.F.d.F. performed experiments and analyzed the data; F.F. analyzed the data; and F.F. and N.F.d.F. wrote the manuscript, with contributions from J.Td.I.S. and L.P.

DECLARATION OF INTERESTS

The authors declare no competing interests

STAR★METHODS

Detailed methods are provided in the online version of this paper and include the following:

- KEY RESOURCES TABLE
- EXPERIMENTAL MODEL AND SUBJECT DETAILS
- METHOD DETAILS
  - AMF colonization phenotyping
  - *Agrobacterium rhizogenes*-mediated transformation
  - RNA extraction and cDNA synthesis
  - Real-Time PCR analysis
  - RNAseq transcriptomic analysis
  - Extraction of strigolactones from roots
  - Detection and quantification of strigolactones
  - *P. ramosa* germination assays
  - Wheat Germ Agglutinin (WGA) Alexafluor-488 staining and confocal microscopy
  - Phylogenetic analyses
- QUANTIFICATION AND STATISTICAL ANALYSIS

SUPPLEMENTAL INFORMATION

Supplemental information can be found online at https://doi.org/10.1016/j.cub.2024.09.058.

Received: December 20, 2023
Revised: July 16, 2024
Accepted: September 23, 2024
Published: October 21, 2024

REFERENCES

1. Imin, N., Mohd-Radzman, N.A., Ogilvie, H.A., and Djordjevic, M.A. (2013). The peptide-encoding CEP1 gene modulates lateral root and nodule numbers in *Medicago truncatula*. J. Exp. Bot. *64*, 5395–5409. https://doi.org/10.1093/jxb/ert369.
2. Mohd-Radzman, N.A., Laffont, C., Ivanovici, A., Patel, N., Reid, D.E., Stougaard, J., Frugier, F., Imin, N., and Djordjevic, M.A. (2016). Different pathways act downstream of the CEP peptide receptor CRA2 to regulate lateral root and nodule development. Plant Physiol. *171*, 2536–2548. https://doi.org/10.1104/pp.16.00113.
3. Laffont, C., Huault, E., Gautrat, P., Endre, G., Kalo, P., Bourion, V., Duc, G., and Frugier, F. (2019). Independent regulation of symbiotic nodulation by the SUNN negative and CRA2 positive systemic pathways. Plant Physiol. *180*, 559–570. https://doi.org/10.1104/pp.18.01588.
4. Gautrat, P., Laffont, C., and Frugier, F. (2020). Compact root architecture 2 promotes root competence for nodulation through the miR2111 systemic effector. Curr. Biol. *30*, 1339–1345.e3. https://doi.org/10.1016/j.cub.2020.01.084.
5. Smith, S.E., Jakobsen, I., Grønlund, M., and Smith, F.A. (2011). Roles of arbuscular Mycorrhizas in plant phosphorus nutrition: interactions between pathways of phosphorus uptake in arbuscular Mycorrhizal roots have important implications for understanding and manipulating plant phosphorus acquisition1. Plant Physiol. *156*, 1050–1057. https://doi.org/10.1104/pp.111.174581.
6. Javot, H., Penmetsa, R.V., Terzaghi, N., Cook, D.R., and Harrison, M.J. (2007). A *Medicago truncatula* phosphate transporter indispensable for the arbuscular mycorrhizal symbiosis. Proc. Natl. Acad. Sci. USA *104*, 1720–1725. https://doi.org/10.1073/pnas.0608136104.
7. Burleigh, S.M., and Harrison, M.J. (1998). Characterization of the *Mt4* gene from *Medicago truncatula*. Gene *216*, 47–53. https://doi.org/10.1016/s0378-1119(98)00326-6.
8. Burleigh, S.H., and Harrison, M.J. (1997). A novel gene whose expression in *Medicago truncatula* roots is suppressed in response to colonization by vesicular-arbuscular mycorrhizal (VAM) fungi and to phosphate nutrition. Plant Mol. Biol. *34*, 199–208. https://doi.org/10.1023/a:1005841119665.
9. Laffont, C., Ivanovici, A., Gautrat, P., Brault, M., Djordjevic, M.A., and Frugier, F. (2020). The NIN transcription factor coordinates CEP and CLE signaling peptides that regulate nodulation antagonistically. Nat. Commun. *11*, 3167. https://doi.org/10.1038/s41467-020-16968-1.
10. Huault, E., Laffont, C., Wen, J., Mysore, K.S., Ratet, P., Duc, G., and Frugier, F. (2014). Local and systemic regulation of plant root system

architecture and symbiotic nodulation by a receptor-like kinase. PLoS Genet. *10*, e1004891. https://doi.org/10.1371/journal.pgen.1004891.

11. Gutjahr, C., and Paszkowski, U. (2013). Multiple control levels of root system remodeling in arbuscular mycorrhizal symbiosis. Front. Plant Sci. *4*, 204. https://doi.org/10.3389/fpls.2013.00204.
12. Parniske, M. (2008). Arbuscular mycorrhiza: the mother of plant root endosymbioses. Nat. Rev. Microbiol. *6*, 763–775. https://doi.org/10.1038/nrmicro1987.
13. Suzuki, W., Konishi, M., and Yanagisawa, S. (2013). The evolutionary events necessary for the emergence of symbiotic nitrogen fixation in legumes may involve a loss of nitrate responsiveness of the NIN transcription factor. Plant Signal. Behav. *8*, e25975. https://doi.org/10.4161/psb.25975.
14. Nishida, H., Tanaka, S., Handa, Y., Ito, M., Sakamoto, Y., Matsunaga, S., Betsuyaku, S., Miura, K., Soyano, T., Kawaguchi, M., et al. (2018). A NIN-LIKE PROTEIN mediates nitrate-induced control of root nodule symbiosis in *Lotus japonicus*. Nat. Commun. *9*, 499. https://doi.org/10.1038/s41467-018-02831-x.
15. Tsikou, D., Yan, Z., Holt, D.B., Abel, N.B., Reid, D.E., Madsen, L.H., Bhasin, H., Sexauer, M., Stougaard, J., and Markmann, K. (2018). Systemic control of legume susceptibility to rhizobial infection by a mobile microRNA. Science *362*, 233–236. https://doi.org/10.1126/science.aat6907.
16. Takahara, M., Magori, S., Soyano, T., Okamoto, S., Yoshida, C., Yano, K., Sato, S., Tabata, S., Yamaguchi, K., Shigenobu, S., et al. (2013). TOO MUCH LOVE, a Novel Kelch Repeat-Containing F-box Protein, Functions in the Long-Distance Regulation of the Legume–Rhizobium Symbiosis. Plant Cell Physiol. *54*, 433–447. https://doi.org/10.1093/pcp/pct022.
17. Gautrat, P., Mortier, V., Laffont, C., De Keyser, A., Fromentin, J., Frugier, F., and Goormachtig, S. (2019). Unraveling new molecular players involved in the autoregulation of nodulation in *Medicago truncatula*. J. Exp. Bot. *70*, 1407–1417. https://doi.org/10.1093/jxb/ery465.
18. Schiessl, K., Lilley, J.L.S., Lee, T., Tamvakis, I., Kohlen, W., Bailey, P.C., Thomas, A., Luptak, J., Ramakrishnan, K., Carpenter, M.D., et al. (2019). NODULE INCEPTION Recruits the Lateral Root Developmental Program for Symbiotic Nodule Organogenesis in *Medicago truncatula*. Curr. Biol. *29*, 3657–3668.e5. https://doi.org/10.1016/j.cub.2019.09.005.
19. Zhu, F., Deng, J., Chen, H., Liu, P., Zheng, L., Ye, Q., Li, R., Brault, M., Wen, J., Frugier, F., et al. (2020). A CEP Peptide Receptor-Like Kinase Regulates Auxin Biosynthesis and Ethylene Signaling to Coordinate Root Growth and Symbiotic Nodulation in *Medicago truncatula*. Plant Cell *32*, 2855–2877. https://doi.org/10.1105/tpc.20.00248.
20. Müller, L.M., Flokova, K., Schnabel, E., Sun, X., Fei, Z., Frugoli, J., Bouwmeester, H.J., and Harrison, M.J. (2019). A CLE-SUNN module regulates strigolactone content and fungal colonization in arbuscular mycorrhiza. Nat. Plants *5*, 933–939. https://doi.org/10.1038/s41477-019-0501-1.
21. Carrï Re, S.B., Verdenaud, M., Gough, C., Gouzy, J.R.M., and Gamas, P. (2020). LeGOO: An Expertized Knowledge Database for the Model Legume *Medicago truncatula*. Plant Cell Physiol. *61*, 203–211. https://doi.org/10.1093/pcp/pcz177.
22. Bravo, A., Brands, M., Wewer, V., Dörmann, P., and Harrison, M.J. (2017). Arbuscular mycorrhiza-specific enzymes FatM and RAM2 fine-tune lipid biosynthesis to promote development of arbuscular mycorrhiza. New Phytol. *214*, 1631–1645. https://doi.org/10.1111/nph.14533.
23. Wang, E., Schornack, S., Marsh, J.F., Gobbato, E., Schwessinger, B., Eastmond, P., Schultze, M., Kamoun, S., and Oldroyd, G.E.D. (2012). A Common Signaling Process that Promotes Mycorrhizal and Oomycete Colonization of Plants. Curr. Biol. *22*, 2242–2246. https://doi.org/10.1016/j.cub.2012.09.043.
24. Zhang, Q., Blaylock, L.A., and Harrison, M.J. (2010). Two *Medicago truncatula* Half-ABC Transporters Are Essential for Arbuscule Development in Arbuscular Mycorrhizal Symbiosis. Plant Cell *22*, 1483–1497. https://doi.org/10.1105/tpc.110.074955.
25. Karlo, M., Boschiero, C., Landerslev, K.G., Blanco, G.S., Wen, J., Mysore, K.S., Dai, X., Zhao, P.X., and de Bang, T.C. (2020). The CLE53–SUNN genetic pathway negatively regulates arbuscular mycorrhiza root colonization in *Medicago truncatula*. J. Exp. Bot. *71*, 4972–4984. https://doi.org/10.1093/jxb/eraa193.
26. Li, X.-R., Sun, J., Albinsky, D., Zarrabian, D., Hull, R., Lee, T., Jarratt-Barnham, E., Chiu, C.H., Jacobsen, A., Soumpourou, E., et al. (2022). Nutrient regulation of lipochitooligosaccharide recognition in plants via NSP1 and NSP2. Nat. Commun. *13*, 6421. https://doi.org/10.1038/s41467-022-33908-3.
27. Huertas, R., Torres-Jerez, I., Curtin, S.J., Scheible, W., and Udvardi, M. (2023). *Medicago truncatula PHO2* genes have distinct roles in phosphorus homeostasis and symbiotic nitrogen fixation. Front. Plant Sci. *14*, 1211107.
28. Aung, K., Lin, S.-I., Wu, C.-C., Huang, Y.-T., Su, C.-L., and Chiou, T.-J. (2006). pho2, a Phosphate Overaccumulator, Is Caused by a Nonsense Mutation in a MicroRNA399 Target Gene. Plant Physiol. *141*, 1000–1011. https://doi.org/10.1104/pp.106.078063.
29. Branscheid, A., Sieh, D., Pant, B.D., May, P., Devers, E.A., Elkrog, A., Schauser, L., Scheible, W.-R., and Krajinski, F. (2010). Expression Pattern Suggests a Role of MiR399 in the Regulation of the Cellular Response to Local Pi Increase During Arbuscular Mycorrhizal Symbiosis. Mol. Plant. Microbe Interact. *23*, 915–926. https://doi.org/10.1094/MPMI-23-7-0915.
30. Wang, P., Snijders, R., Kohlen, W., Liu, J., Bisseling, T., and Limpens, E. (2021). Medicago SPX1 and SPX3 regulate phosphate homeostasis, mycorrhizal colonization, and arbuscule degradation. Plant Cell *33*, 3470–3486. https://doi.org/10.1093/plcell/koab206.
31. Shi, J., Zhao, B., Zheng, S., Zhang, X., Wang, X., Dong, W., Xie, Q., Wang, G., Xiao, Y., Chen, F., et al. (2021). A phosphate starvation response-centered network regulates mycorrhizal symbiosis. Cell *184*, 5527–5540.e18. https://doi.org/10.1016/j.cell.2021.09.030.
32. Das, D., Paries, M., Hobecker, K., Gigl, M., Dawid, C., Lam, H.-M., Zhang, J., Chen, M., and Gutjahr, C. (2022). PHOSPHATE STARVATION RESPONSE transcription factors enable arbuscular mycorrhiza symbiosis. Nat. Commun. *13*, 477. https://doi.org/10.1038/s41467-022-27976-8.
33. Yuan, K., Zhang, H., Yu, C., Luo, N., Yan, J., Zheng, S., Hu, Q., Zhang, D., Kou, L., Meng, X., et al. (2023). Low phosphorus promotes NSP1-NSP2 heterodimerization to enhance strigolactone biosynthesis and regulate shoot and root architecture in rice. Mol. Plant *16*, 1811–1831. https://doi.org/10.1016/j.molp.2023.09.022.
34. Tokunaga, T., Hayashi, H., and Akiyama, K. (2015). Medicaol, a strigolactone identified as a putative didehydro-orobanchol isomer, from *Medicago truncatula*. Phytochemistry *111*, 91–97. https://doi.org/10.1016/j.phytochem.2014.12.024.
35. Akiyama, K., Matsuzaki, K., and Hayashi, H. (2005). Plant sesquiterpenes induce hyphal branching in arbuscular mycorrhizal fungi. Nature *435*, 824–827. https://doi.org/10.1038/nature03608.
36. Gomez-Roldan, V., Fermas, S., Brewer, P.B., Puech-Pagès, V., Dun, E.A., Pillot, J.-P., Letisse, F., Matusova, R., Danoun, S., Portais, J.-C., et al. (2008). Strigolactone inhibition of shoot branching. Nature *455*, 189–194. https://doi.org/10.1038/nature07271.
37. Cardoso, C., Ruyter-Spira, C., and Bouwmeester, H.J. (2011). Strigolactones and root infestation by plant-parasitic *Striga, Orobanche* and *Phelipanche* spp. Plant Sci. *180*, 414–420. https://doi.org/10.1016/j.plantsci.2010.11.007.
38. Boisson-Dernier, A., Chabaud, M., Garcia, F., Bécard, G., Rosenberg, C., and Barker, D.G. (2001). *Agrobacterium rhizogenes*-Transformed Roots of *Medicago truncatula* for the Study of Nitrogen-Fixing and Endomycorrhizal Symbiotic Associations. Mol. Plant Microbe Interact. *14*, 695–700. https://doi.org/10.1094/MPMI.2001.14.6.695.
39. Pecrix, Y., Staton, S.E., Sallet, E., Lelandais-Brière, C., Moreau, S., Carrère, S., Blein, T., Jardinaud, M.F., Latrasse, D., Zouine, M., et al. (2018). Whole-genome landscape of *Medicago truncatula* symbiotic

genes. Nat. Plants *4*, 1017–1025. https://doi.org/10.1038/s41477-018-0286-7.

40. Hoffmann, B., Trinh, T.H., Leung, J., Kondorosi, A., and Kondorosi, E. (1997). A New *Medicago truncatula* Line with Superior in Vitro Regeneration, Transformation, and Symbiotic Properties Isolated Through Cell Culture Selection. MPMI *10*, 307–315. https://doi.org/10.1094/MPMI.1997.10.3.307.
41. Martinez, L., Pouvreau, J.-B., Montiel, G., Jestin, C., Delavault, P., Simier, P., and Poulin, L. (2023). Soil microbiota promotes early developmental stages of *Phelipanche ramosa* L. Pomel during plant parasitism on *Brassica napus* L. Plant Soil *483*, 667–691. https://doi.org/10.1007/s11104-022-05822-6.
42. Karimi, M., Inzé, D., and Depicker, A. (2002). GATEWAY vectors for Agrobacterium-mediated plant transformation. Trends Plant Sci. *7*, 193–195. https://doi.org/10.1016/s1360-1385(02)02251-3.
43. Rich, M.K., Vigneron, N., Libourel, C., Keller, J., Xue, L., Hajheidari, M., Radhakrishnan, G.V., Le Ru, A., Diop, S.I., Potente, G., et al. (2021). Lipid exchanges drove the evolution of mutualism during plant terrestrialization. Science *372*, 864–868. https://doi.org/10.1126/science.abg0929.
44. Katoh, K., Rozewicki, J., and Yamada, K.D. (2019). MAFFT online service: multiple sequence alignment, interactive sequence choice and visualization. Brief. Bioinform. *20*, 1160–1166. https://doi.org/10.1093/bib/bbx108.
45. Hewitt, E.J. (1953). Sand and Water Culture Methods Used in the Study of Plant Nutrition. Soil Sci. Soc. Am. J. *17*, 301. https://doi.org/10.2136/sssaj1953.03615995001700030033x.
46. Vierheilig, H., Coughlan, A.P., Wyss, U., and Piche, Y. (1998). Ink and vinegar, a simple staining technique for arbuscular-mycorrhizal fungi. Appl. Environ. Microbiol. *64*, 5004–5007.
47. Mcgonigle, T.P., Miller, M.H., Evans, D.G., Fairchild, G.L., and Swan, J.A. (1990). A new method which gives an objective measure of colonization of roots by vesicular—arbuscular mycorrhizal fungi. New Phytol. *115*, 495–501. https://doi.org/10.1111/j.1469-8137.1990.tb00476.x.
48. Fahraeus, G. (1957). The infection of clover root hairs by nodule bacteria studied by a simple glass slide technique. J. Gen. Microbiol. *16*, 374–381. https://doi.org/10.1099/00221287-16-2-374.
49. Proust, H., Bazin, J., Sorin, C., Hartmann, C., Crespi, M., and Lelandais-Brière, C. (2018). Stable Inactivation of MicroRNAs in Medicago truncatula Roots. In Functional Genomics in *Medicago truncatula*: Methods and Protocols Methods in Molecular Biology, L.A. Cañas, and J.P. Beltrán, eds. (Springer), pp. 123–132. https://doi.org/10.1007/978-1-4939-8633-0_9.
50. Feddermann, N., Boller, T., Salzer, P., Elfstrand, S., Wiemken, A., and Elfstrand, M. (2008). *Medicago truncatula* shows distinct patterns of mycorrhiza-related gene expression after inoculation with three different arbuscular mycorrhizal fungi. Planta *227*, 671–680. https://doi.org/10.1007/s00425-007-0649-1.
51. Gonzalez-Rizzo, S., Crespi, M., and Frugier, F. (2006). The *Medicago truncatula* CRE1 cytokinin receptor regulates lateral root development and early symbiotic interaction with *Sinorhizobium meliloti*. Plant Cell *18*, 2680–2693. https://doi.org/10.1105/tpc.106.043778.
52. McCarthy, D.J., Chen, Y., and Smyth, G.K. (2012). Differential expression analysis of multifactor RNA-Seq experiments with respect to biological variation. Nucleic Acids Res. *40*, 4288–4297. https://doi.org/10.1093/nar/gks042.
53. Ge, S.X., Jung, D., and Yao, R. (2020). ShinyGO: a graphical gene-set enrichment tool for animals and plants. Bioinformatics *36*, 2628–2629.
54. Oliveros, J.C. (2007). VENNY. An interactive tool for comparing lists with Venn diagrams. http://bioinfogp.cnb.csic.es/tools/venny/index.html.
55. Liu, W., Kohlen, W., Lillo, A., op den Camp, R., Ivanov, S., Hartog, M., Limpens, E., Jamil, M., Smaczniak, C., Kaufmann, K., et al. (2011). Strigolactone Biosynthesis in *Medicago truncatula* and Rice Requires the Symbiotic GRAS-Type Transcription Factors NSP1 and NSP2. Plant Cell *23*, 3853–3865. https://doi.org/10.1105/tpc.111.089771.
56. Volpe, V., Chialva, M., Mazzarella, T., Crosino, A., Capitanio, S., Costamagna, L., Kohlen, W., and Genre, A. (2023). Long-lasting impact of chitooligosaccharide application on strigolactone biosynthesis and fungal accommodation promotes arbuscular mycorrhiza in *Medicago truncatula*. New Phytol. *237*, 2316–2331. https://doi.org/10.1111/nph.18697.
57. Lechat, M.-M., Brun, G., Montiel, G., Véronési, C., Simier, P., Thoiron, S., Pouvreau, J.-B., and Delavault, P. (2015). Seed response to strigolactone is controlled by abscisic acid-independent DNA methylation in the obligate root parasitic plant, *Phelipanche ramosa* L. Pomel. J. Exp. Bot. *66*, 3129–3140. https://doi.org/10.1093/jxb/erv119.
58. Pouvreau, J.-B., Gaudin, Z., Auger, B., Lechat, M.-M., Gauthier, M., Delavault, P., and Simier, P. (2013). A high-throughput seed germination assay for root parasitic plants. Plant Methods *9*, 32. https://doi.org/10.1186/1746-4811-9-32.
59. de Bang, T.C., Lundquist, P.K., Dai, X., Boschiero, C., Zhuang, Z., Pant, P., Torres-Jerez, I., Roy, S., Nogales, J., Veerappan, V., et al. (2017). Genome-Wide Identification of *Medicago* Peptides Involved in Macronutrient Responses and Nodulation. Plant Physiol. *175*, 1669–1689. https://doi.org/10.1104/pp.17.01096.
60. Robinson, O., Dylus, D., and Dessimoz, C. (2016). Phylo.io: Interactive Viewing and Comparison of Large Phylogenetic Trees on the Web. Mol. Biol. Evol. *33*, 2163–2166. https://doi.org/10.1093/molbev/msw080.

STAR★METHODS

KEY RESOURCES TABLE

REAGENT or RESOURCE	SOURCE	IDENTIFIER
Bacterial and virus strains		
Rhizophagus irregularis DAOM 197198	Agronutrition https://www.agronutrition.com/	AP2007-A
Escherichia coli DH5α	ThermoFisher Scientific https://www.thermofisher.com	Cat#18258012
Agrobacterium rhizogenes Arqua1	Boisson-Dernier et al.[38]	Lab#Arqua1
Chemicals, peptides, and recombinant proteins		
rac-GR24	Chiralix https://www.chiralix.com/	CX23880
WGA AlexaFluor 488	ThermoFisher Scientific https://www.thermofisher.com	W11261
Methylthiazolyldiphenyl-tetrazolium bromide (MTT)	Sigma Aldrich https://www.sigmaaldrich.com/	M2128
Critical commercial assays		
Quick-RNA Miniprep Kit	Zymo Research https://www.zymoresearch.com	Cat#R1055
SuperScript III Reverse Transcriptase	ThermoFisher Scientific https://www.thermofisher.com	Cat#18080044
LightCycler 480 SYBR Green I Master Mix	Roche https://lifescience.roche.com	Cat#04887352001
Sheaffer black ink	Sheaffer https://sheaffer.com/	Sheaffer Skrip
Deposited data		
RNA-seq datasets	This paper	NCBI SRA: PRJNA1156341
Experimental models: Organisms/strains		
Medicago truncatula Jemalong A17	Pecrix et al.[39]	Lab#MtJemA17
Medicago truncatula R108	Hoffmann et al.[40]	Lab#MtR108
Medicago truncatula cra2-11	Laffont et al.[3]	Lab#MtJem*cra2-11*
Medicago truncatula cra2-1	Huault et al.[10]	Lab#MtJem*cra2-1*
Phelipanche ramose	Martinez et al.[41]	Lab#Pram123
Oligonucleotides		
Listed in Table S4	Eurofins https://www.eurofinsgenomics.eu/	Oligos IDs listed in Table S4
Recombinant DNA		
pK7WG2D Empty Vector	Karimi et al.[42]	Lab#pK7WG2D-empty
p35S:*CEP1*	Imin et al.[1]	Lab#pK7WG2D-OECEP1
p2L-50507 Empty Vector	Rich et al.[43]	Lab#50507-empty
p35S:*CEP2*	this study	Lab#50507-empty
Software and algorithms		
XLStat	Xlstat https://www.xlstat.com/	Xlstat-Basic-v17.06
R	R project https://www.r-project.org/	N/A
ShinyGO	ShinyGo http://shiny.chemgrid.org/boxplotr/	N/A
Venny	Venny https://bioinfogp.cnb.csic.es/tools/venny/	N/A
MAFFT v7.407	Katoh et al.[44]	N/A
Other		
LEGoo	https://lipm-browsers.toulouse.inra.fr/k/legoo/	N/A

EXPERIMENTAL MODEL AND SUBJECT DETAILS

The *Medicago truncatula* Jemalong A17[39] and R108[40] genotypes, the *cra2*-1 and *cra2*-11 mutants that contain respectively a *Tnt1* retro-transposon insertion in the leucine-rich repeat region or in the kinase domain encoding region (key resources table) were used in this study. Seeds were scarified with 95-98% sulfuric acid (Sigma-Aldrich) during eight minutes and washed five times with water. They were then surface sterilized with bleach (9.5%) for one min, washed again six times with sterilized water, and transferred onto 10% w/v water-agar (Sigma # A9799) solid medium plates. The plates were kept in the dark at 4°C for 24h, and then transferred at 24°C overnight for germination.

For contrasting Pi availability experiments, plants were grown in the following different conditions without AMF inoculation: 0.5X Long Ashton medium[45] modified with low (7.5 μM) or high (2 mM) Pi (NaH_2PO_4) in pots containing a mix of zeolite 1.0-2.5 mm and zeolite 0.5-1.0 mm fractions (v/v) as substrate (Symbiom). Plants were grown with a 16h photoperiod and 160 μE light intensity, at 24°C, and with 60% of relative humidity.

For inoculation with AMF, plants were grown in pots containing a mix of zeolite 1.0-2.5 mm and zeolite 0.5-1.0 mm fractions (v/v) as substrate (Symbiom), watered twice a week with 0.5X Long Ashton medium[45] containing 7.5 μM NaH_2PO_4, and inoculated directly after germination with 300 spores of the *Rhizophagus irregularis* DAOM 197198 strain (Agronutrition; key resources table). Roots were harvested six weeks after AMF inoculation and washed three time with water before staining (see below).

For root exudate collection, plants were grown for four weeks under the low Pi condition described above. Five plants per genotype were removed from the substrate, their root system rinsed with water, and plants were then transferred in 50 mL Falcon tubes with 20 mL of water and shoots outside the open tube. After 24h, plants were removed and the water containing root exudates was sterilized with a 0.2 μm filter and further used, pure or diluted with water, for germination assays with *Phelipanche ramosa*[41] seeds (key resources table).

METHOD DETAILS

AMF colonization phenotyping

Whole plant root systems were collected six weeks after AMF inoculation, washed with water, treated with 10% KOH for two days at room temperature, washed again with water, and finally stained with an ink solution (5% Schaeffer black ink, 95% acetic acid; key resources table) for 5 min at 95°C.[46] Stained roots were then washed again with water, and cleared with 50% ethanol.

The quantification of mycorrhizal colonization was performed using the grid-intersect method.[47] Entire root systems were cut into small fragments (~2 cm) and randomized under the microscope. A minimal WT plant root colonization of approximately 50% was validated in all independent experiments before proceeding to the detailed quantifications. At least 400 root intersections were observed for each plant root system (n = 8-10 per genotype) to quantify root apices, fungal infection points at the root epidermis (hyphopodia), as well as arbuscules and intraradical mycelium colonization of the root cortex. Observations were performed with a S6E microscope (Leica microsystems).

Agrobacterium rhizogenes-mediated transformation

The p35S:*CEP1* construct, as well as the control empty vector pK7WG2D,[42] were generated in Imin et al.[1]; key resources table), and used for root transformation using the *Agrobacterium rhizogenes* Arqua1 strain (key resources table), as described in Boisson-Dernier et al.[38] The p35S:*CEP2* construct was generated in the p2L-50507 plasmid,[43] and the p2L-50507 plasmid was used as control empty vector. Composite plants, with WT (A17) shoots and transgenic roots, were grown *in vitro* on Fahraeus medium[48] plates and inoculated with AMF as described above.

RNA extraction and cDNA synthesis

Total RNAs were extracted using the Quick-RNA Miniprep kit (Zymo, key resources table), from roots which were collected on plants grown in low *versus* high Pi conditions four weeks after germination, or six weeks after inoculation with the AMF. In all cases, pools of three plants were used as biological replicates. The DNAse treatment was performed with a RNAse-free DNAse1 following the manufacturer instructions. cDNAs were then obtained with the Reverse Transcriptase Superscript III (Invitrogen; 200 U/μL; key resources table) following manufacturer instructions. A Stem-Loop Reverse Transcription (RT) was performed to amplify selected mature 21 base pairs miRNAs thanks to dedicated adapters (Table S4), as described in Proust et al.[49]

Real-Time PCR analysis

Gene expression was analyzed by quantitative RT-PCR (qRT-PCR) on a LightCycler96 apparatus (Roche) using the Light Cycler 480 Green I Master mix (Roche, key resources table) and specific primers to amplify the genes of interest (listed in Table S4). Forty-five cycles of amplification (15 sec at 95°C, 15 sec at 60°C, 15 sec at 72°C) were performed, with a final melting curve step (from 60 to 95°C) to assess primers specificity. All primers used were selected with an efficiency of at least 90%. Mycorrhizal and Pi starvation marker genes were respectively described in Feddermann et al.[50] and Branscheid et al.[29] Gene expression normalizations were performed with the reference genes *MtActin11* (*MtACT11*) and *MtRBP1*, and with the miR162 for mature miRNAs, based on previous studies.[4,51] As the normalization with *MtACT11* or *MtRBP1* gave similar results, only the normalization with *MtACT11* is shown in figures.

RNAseq transcriptomic analysis

Total RNAs were extracted using the ZYMO DirectZol RNA Miniprep kit, following manufacturer's instructions. RNA samples were quantified using Qubit 4.0 Fluorometer (Life Technologies, Carlsbad, CA, USA) and RNA integrity was checked with RNA Kit on Agilent 5600 Fragment Analyzer (Agilent Technologies, Palo Alto, CA, USA).

RNA sequencing libraries were prepared using the NEB Next Ultra II RNA Library Prep Kit for Illumina following manufacturer's instructions (NEB, Ipswich, MA, USA). Briefly, mRNAs were first enriched with Oligo(dT) beads. Enriched mRNAs were fragmented for 15 minutes at 94 °C.

First strand and second strand cDNAs were subsequently synthesized. cDNA fragments were end repaired and adenylated at 3'ends, and universal adapters were ligated to cDNA fragments, followed by index addition and library enrichment by limited-cycle PCR. Sequencing libraries were validated using NGS Kit on the Agilent 5300 Fragment Analyzer (Agilent Technologies,

Palo Alto, CA, USA), and quantified by using Qubit 4.0 Fluorometer (Invitrogen, Carlsbad, CA).

The sequencing libraries were multiplexed and clustered on the flowcell. After clustering, the flowcell was loaded on the Illumina NovaSeq instrument according to manufacturer's instructions.

The samples were sequenced using a 2x150 Pair-End (PE) configuration. Image analysis and base calling were conducted by the NovaSeq Control Software v1.8.1 on the NovaSeq instrument. Raw sequence data (.bcl files) generated from Illumina NovaSeq was converted into fastq files and de- multiplexed using Illumina bcl2fastq program version 2.20. One mismatch was allowed for index sequence identification.

To perform differential analyses, htseq-counts files (Genewiz, Azenta Life Sciences) mapped onto the v5 version of the *M. truncatula* genome[39] were analyzed with the R software using the EdgeR package version 3.24.3[52] (key resources table). Gene annotations from the LeGOO database were used[21] (key resources table). Genes which did not have at least one read after a count per million in at least one half of the samples were discarded at first. Then, raw counts were normalized using the Trimmed Mean of M-values method. The count distribution was modelled with a negative binomial generalized linear model where the condition, the genotype and the interaction between conditions and genotypes were taken into account, and where the dispersion was estimated with the EdgeR method.[52] A likelihood ratio test was performed to evaluate the effect of the condition in each genotype, or the effect of the genotype in each condition. Raw P values were adjusted with the Benjamini–Hochberg procedure to control the False Discovery Rate (FDR). A gene was declared as differentially expressed if its adjusted P value was ≤ 0.05.

GO term enrichments were determined using the ShinyGO web tool[53] (key resources table) with default parameters, and Venny[54] (key resources table) was used to perform Venn diagrams.

Extraction of strigolactones from roots

For the SL content analysis, 500 mg of ground roots (six-week-old plants grown in low Pi) were transferred to 10 mL glass vials. SLs were extracted with 2 mL of ethyl acetate containing 10^{-8} M GR24 (Chiralix, key resources table) as an internal standard (final concentration 10^{-7} M). Vials were vortexed, sonicated for 20 s (Branson Ultrasonics sonication bath; Emerson Automation Solutions, Busseno, Italy), and extracted at 4°C overnight on an orbital shaker. Samples were centrifuged for 10 min at 2500g at room temperature. Organic phases were transferred to 4 mL glass vials, and the solvent was evaporated using a speed vacuum system (SPD121P; ThermoSavant, Hastings, UK). SL from roots were quantified according to Liu et al.[55]

Detection and quantification of strigolactones

Sample residues were dissolved in 100 μL of acetone/water (30:70, v/v) and filtered through a 0.45 mm Minisart SRP4 filter (Sartorius, Goettingen, Germany). The SL analysis was performed by comparing retention times and mass transitions as previously described by Volpe et al.,[56] with modifications. A Waters Xevo TQs mass spectrometer with an electrospray ionization source coupled to an Acquity UPLC system (Waters, Milford, USA) was used. Chromatographic separations were conducted on an Acquity UPLC BEH C18 column (100 mm, 2.1 mm, 1.7 mm; Waters, USA) using an acetonitrile/water (0.1% formic acid) gradient. The column was operated at 50°C with a flow rate of 0.5 mL/min. The gradient started at 5% (v/v) acetonitrile for 0.67 min, increased to 27% at 5 min, and to 65% at 8 min. The gradient then increased to 90% acetonitrile in 0.5 min, was maintained for 1 min, before returning to 5% for 2.5 min. The sample injection volume was 5 μL. The mass spectrometer was operated in the positive electrospray ionization mode, with cone and desolvation gas flows set to 150 and 1000 l/h, respectively. The capillary voltage was 2.5 kV, source temperature 150°C, and desolvation temperature 500°C. Argon was used for fragmentation by collision-induced dissociation. Multiple Reaction Monitoring (MRM) was used for quantification. MRM transitions, cone voltage, and collision energy for didehydroorobanchol and GR24 were described by Volpe et al.[56]

P. ramosa germination assays

P. ramosa seeds (key resources table) were surface-sterilized in a 2.4% sodium hypochlorite solution for 4 min under gentle stirring, then rinsed three times for 5 min with sterile distilled water using a cell strainer (EASYstrainer 40 μm, Greiner). Seeds were suspended at a final concentration of 5 g/L in a conditioning solution (1 mM 4-(2-hydroxyethyl)-1-piperazineethanesulfonic acid (HEPES), pH 7.5 adjusted with KOH; PPM 0.1% v/v) and incubated in the dark at 21°C for 14 days, as described in Lechat et al.[57] Germination was induced in 96-well plates by adding 50 μL of serial dilutions of fresh *M. truncatula* root exudates to 50 μL of conditioned seeds (~75 seeds per well). Water and acetonitrile, and a 10^{-7} M rac-GR24 treatment (in 0.001% acetonitrile; Chiralix, key resources table) served as two negative and one positive controls, respectively. After six days of incubation at 21°C in the dark, seeds were stained with 10 μL of 5 g/L methylthiazolyldiphenyl-tetrazolium bromide (MTT; Sigma-Aldrich) to facilitate counting.[58] The germination rate was assessed one day later under a binocular magnifier (Leica MZ10F).

Wheat Germ Agglutinin (WGA) Alexafluor-488 staining and confocal microscopy

For WGA AlexaFluor-488 staining, six-week-old mycorrhized *M. truncatula* A17 and *cra2*-11 root systems were incubated in a 10% KOH solution for 48 h at room temperature. Following this treatment, *M. truncatula* roots were then incubated with 0.1% Triton X-100 for 1 h, and finally in 1 μg/mL WGA Alexafluor-488 (key resources table) solution diluted in PBS 1x at 4°C for 48 hours. The roots were

kept in the dark, wrapped in a paper foil, and stored at 4°C before imaging. Stained roots were observed with an upright laser scanning confocal microscope (SP8 Leica Microsystems). WGA-Alexafluor-488 was detected using a 488 nm laser and the emitted light was collected under a 498-550 nm window.

Phylogenetic analyses

The phylogenetic analysis of CEP and PIP pre-proprotein sequences, recovered from the de Bang et al. study,[59] were aligned using the MAFFT[44] (Multiple sequence Alignment based on the Fast Fourier Transform; key resources table) method using default parameters. The tree was then constructed by average linkage using the unweighted pair group method with arithmetic means, and displayed using the MAFFT phylo.io tool.[60]

QUANTIFICATION AND STATISTICAL ANALYSIS

Statistical analyses were performed with the XLSTAT software or using dedicated R scripts (key resources table). The normal distribution of experimental values was determined with a Shapiro test ($P < 0.05$). Statistical difference between groups (low Pi *versus* high Pi, WT *versus cra2* mutant, empty vector *versus* 35S:*MtCEP1/MtCEP2* roots) was then determined using a Student's t test when data were normally distributed, or a Wilcoxon test when data were not normally distributed. All of the statistical details of experiments can be found in the Figure legends.